SERI/TP-217-3394
UC Category: 261
DE89000834

Prediction of Stochastic Blade Responses Using Measured Wind-Speed Data as Input to the FLAP Code

A. D. Wright
R. W. Thresher

November 1988

Prepared for the Eighth ASME
Wind Energy Symposium
Houston, Texas
22-25 January 1989

Prepared under Task No. WE811203

Solar Energy Research Institute
A Division of Midwest Research Institute

1617 Cole Boulevard
Golden, Colorado 80401-3393

Prepared for the
U.S. Department of Energy
Contract No. DE-AC02-83CH10093

NOTICE

Printed in the United States of America
Available from:
National Technical Information Service
U.S. Department of Commerce
5285 Port Royal Road
Springfield, VA 22161

Price: Microfiche A01
Printed Copy A02

Codes are used for pricing all publications. The code is determined by the number of pages in the publication. Information pertaining to the pricing codes can be found in the current issue of the following publications which are generally available in most libraries: *Energy Research Abstracts (ERA)*; *Government Reports Announcements* and Index (*GRA* and I); *Scientific and Technical Abstract Reports (STAR)*; and publication NTIS-PR-360 available from NTIS at the above address.

SERI

PREDICTION OF STOCHASTIC BLADE RESPONSES USING MEASURED WIND-SPEED DATA AS INPUT TO THE FLAP CODE

A.D. Wright
R.W. Thresher

Solar Energy Research Institute
Golden, CO

ABSTRACT

Accurately predicting wind turbine blade loads and response is important in predicting the fatigue life of wind turbines. The necessity of including turbulent wind effects in structural dynamics models has long been recognized. At SERI, the structural dynamics model, or FLAP (Force and Loads Analysis Program), is being modified to include turbulent wind fluctuations in predicting rotor blade forces and moments.

The objective of this paper is to show FLAP code predictions compared to measured blade loads, using actual anemometer array data and a curve-fitting routine to form series expansion coefficients as the turbulence input to FLAP. The predictions are performed for a three-bladed upwind field test turbine. An array of nine anemometers was located 0.8 rotor diameters (D) upwind of the turbine, and data from each anemometer are used in a least-squares curve-fitting routine to obtain a series expansion of the turbulence field over the rotor disk.

Three 10-min data cases are used to compare FLAP predictions to measured results. Each case represents a different mean wind speed and turbulence intensity. The time series of coefficients in the expansion of the turbulent velocity field are input to the FLAP code. Time series of predicted flap-bending moments at two blade radial stations are obtained, and power spectra of the predictions are then compared to power spectra of the measured blade bending moments. Conclusions are then drawn about the FLAP code's ability to predict the blade loads for these three data cases. Recommendations for future work are also made.

NOMENCLATURE

Hz	hertz
ft	feet
D	rotor diameter
EI	blade stiffness distribution (Figure 2)
P	cycles per revolution
m	meters
r	blade radial coordinate
R	rotor disk radius
t	time
V_{disk}	disk averaged wind speed
$\bar{V}$	mean wind speed
$\bar{V}_i$	10-min average of data from anemometer #i
V_{ni}	time-series data for anemometer #i (n^{th} data point)
v_{ni}	residual time-series data for anemometer #i
$V_y(r,\psi,t)$	wind-speed component normal to the rotor disk
$V_{y,o}(t)$	coefficient in wind-speed series expansion: mean component
$V_{y,z}(t)$	coefficient in wind-speed series expansion: component associated with vertical linear shear
$V_{y,x}(t)$	coefficient in wind-speed series expansion: component associated with horizontal linear shear
$V_{y,rr}(t)$, $V_{y,rc}(t)$, $V_{y,rs}(t)$	higher-order series expansion terms (associated with quadratic terms)

W	blade weight distribution (Figure 2)
x	horizontal direction (see Figure 4)
z	vertical direction (see Figure 4)
ψ	blade azimuth angle
σ	standard deviation

INTRODUCTION

Past comparisons of wind turbine blade load predictions with test results have indicated large discrepancies. These discrepancies are thought to be caused by turbulent wind fluctuations, which have not been accounted for in structural dynamics models.

In a previous paper (1), deterministic loads prediction from the FLAP code were compared to measured results for the Howden 330-kW wind turbine in Palm Springs, California. Good agreement for the deterministic loads was obtained between predictions and experimental data, provided the wind-shear velocity profile was accurately input to the FLAP code.

The necessity of including turbulent wind effects in structural dynamics models is now widely recognized. The subject of stochastic loads for wind turbines remained largely unreported until the early 1980s. The 1981 Wind Turbine Dynamics Workshop, held in Cleveland, Ohio, marked the beginning of a number of papers and presentations concerning the simulation of atmospheric turbulence and the prediction of turbulence-induced blade loads. In (2), a simplified treatment of turbulence was developed to predict the response characteristics of horizontal-axis wind turbines (HAWTs) to turbulence. The filtered noise model described in (2) has been further refined for use in structural dynamics models (3,4).

Recently, turbulence-induced blade loads for the Howden 330-kW turbine have been reported (5). In (5), a model was presented that accounted for the dominant vibration mode of the blade and also used the experimentally determined wind spectra and coherence functions at a fixed point in space. This model works in the frequency domain, and results for the flap-bending moments were compared to measured results. The results agreed well with measured data, especially below rated wind speeds. Recently, a method for performing a three-dimensional wind simulation has also been reported (6).

A companion paper (7) to this paper describes the filtered noise model (4) incorporated into the FLAP dynamics code. Predicted blade bending moments are compared to measured results for different cases for the Howden 330-kW field test turbine in Palm Springs, California. Inputs to the code include parameters such as the mean wind speed, turbulence intensity, and integral scale.

In this paper, wind-speed data from an array of nine anemometers, located 0.8 D upwind of the Howden 330-kW turbine, are used as turbulence excitation in FLAP. Data from the array of anemometers are used in a least-squares curve-fitting routine to obtain a series expansion of the turbulent wind profile over the rotor disk. The coefficients of this expansion are computed for each measurement interval of recorded wind data. The time series of coefficients is then input to the FLAP code. Blade flapwise bending moments are then computed for the stochastic portion of blade response by setting deterministic excitations to zero in FLAP. The deterministic portion of blade response is subtracted from the test data by the process of azimuth averaging. The deterministic blade load comparisons for this machine were previously reported in (1).

First, a description of the Howden 330-kW machine is given. Then, the method of inputting the turbulent wind fluctuations to FLAP is shown. Three 10-min data cases are used for comparison cases, and each has a different mean wind speed and turbulence intensity.

Power spectra of predicted flapwise bending moments of two different blade spanwise locations are compared to measured results for the stochastic portion of blade response. Conclusions are drawn as to the code's predictive capability.

TURBINE DESCRIPTION

As part of the DOE Cooperative Field Test Program, the Solar Energy Research Institute (SERI) and Southern California Edison (SCE) carried out a comprehensive field measurement program on the SCE-owned, 330-kW HAWT located near Palm Springs, California, in San Gorgonio Pass. The measurement program included a complement of structural load measurements to characterize the dynamic response of the turbine, as well as an array of wind sensors to characterize both the mean and turbulent wind field in front of the turbine.

The field test turbine, manufactured by James Howden and Company, was a three-bladed, upwind machine with a rigid hub and wood/epoxy blades. It was rated at 330 kW in a hub-height wind speed of 32.4 mph (14.5 m/s) and was designed to operate in cut-in and cut-out wind speeds of 13.4 and 62.6 mph (6.0 and 28.0 m/s), respectively. The rotor diameter was 85.3 ft (26 m) and the rotor speed was 42 rpm. The blades were tapered and twisted, with a maximum chord of 4.8 ft (1.47 m) and a maximum twist angle of 16°; the blade tapered to a 2.6-ft (0.8-m) chord and 0° twist at the blade tip. The blade airfoil section was a GA(W)-1, 17% thick. The blade dimensions are shown in Table 1.

The rotor axis centerline above the ground was at 79.1 ft (24.1 m), and the rotor coning angle (precone) was 0°. The tower diameter was 5.9 ft (1.8 m), and the distance from the yaw axis to the rotor plane was 11.5 ft (3.5 m). Figure 1 is a sketch of the turbine.

In modeling the dynamic response of the blade correctly, the distributed weight and stiffness distribution of the blade are important parameters. Figure 2 shows these distributions. To obtain good predictive capabilities with any type of dynamic model, the natural frequencies of the model must faithfully reproduce those of the physical system. The predicted natural frequencies for the turbine are listed in Table 2 as

Table 1. Howden Wind Turbine Blade Dimensions [from (8)]

Radius (ft)	Chord (ft)	Twist* (deg)	Notes
1.31	2.10	16.0	Root (fixed pitch)
9.84	4.80	16.0	Blade "knee"
36.10	3.10	3.2	Tip joint
42.60	2.60	0.0	Tip (pitchable)

*Toward feather.

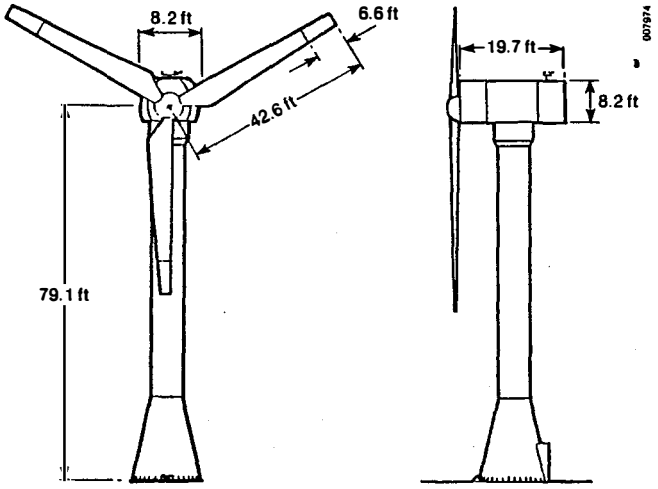

Fig. 1. The Howden HWP 330/26 wind turbine

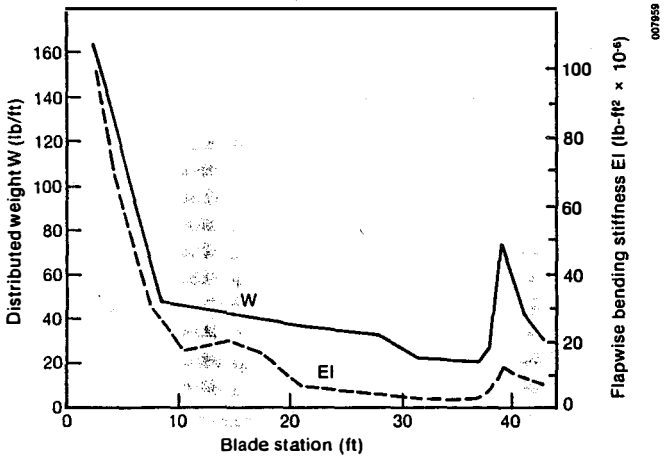

Fig. 2. Weight and stiffness distribution for the Howden 42.6-ft wood/epoxy blade

computed by Howden (8). For more information on these combined rotor/tower modes, see (8).

Table 2 shows that there are several natural frequencies quite close to a frequency of two times the rotor passage frequency (2 P). Because FLAP does not account for tower motion, it was impossible to model the actual blade/tower interactions of the turbine. To make a simple approximation for this situation, only the first blade flapwise bending mode was used to model the blade flapping response. Using the data inputs for mass and stiffness distribution caused FLAP to overestimate the first flapwise natural frequency. The frequency was thus lowered to 1.40 Hz (2 P). This covered the closely spaced natural frequencies near 1.40 Hz and disregarded the higher frequencies.

The mass and stiffness distributions of Figure 2 were used as a starting approximation. Then, the resulting modal stiffness coefficient computed by the FLAP code was manually adjusted to set the blade rotating natural frequency at 1.40 Hz (2 P). The modal mass coefficient was not changed, so that the centrifugal forces on the blade would be accurately computed. Structural damping was not included in the model; only

Table 2. Predicted Natural Frequencies (Nonrotating) of the Howden 330-kW Wind Turbine [from (8)].

Mode	Frequency		Mode Shape
	Hz	P*	
1	1.33	1.90	Rotor flap (tower, fore to aft)
2	1.43	2.04	Rotor flap (no tower)
3	1.44	2.04	Rotor flap (no tower)
4	1.53	2.20	Tower (rotor, side to side)
5	1.72	2.50	Rotor flap (tower, fore to aft)
6	3.43	4.90	Blade flap

*Cycles per revolution

aerodynamic damping due to blade flapping response was included.

INSTRUMENTATION

A total of 44 channels of data were recorded in multiplexed form on a Honeywell 101 14-channel tape recorder. Thirteen channels of machine data were collected through the Howden data system. The effective cut-off frequency of the Howden data system was about 30 Hz. The 31 channels of atmospheric data were low-pass filtered at 10 Hz. The wind data of interest for this study came from the vertical-plane array using three-axis UVW Gill propeller anemometers located 68.9 ft (21 m) or 0.8 D due west and upwind of the turbine in the prevailing wind direction. The numbering scheme for the anemometers on this array is shown in Figure 3. In addition, there was a single UVW Gill propeller anemometer at hub height, located 2 D upwind. Data were analyzed from strain gages located at the root and at the 27.1-ft (8.25-m) station on the blade. The analog data collected during the test were digitized at SERI using the NEFF 720 system at a sample rate of 20.84 Hz. This high rate was necessary to accurately resolve the blade angular position for azimuth averaging.

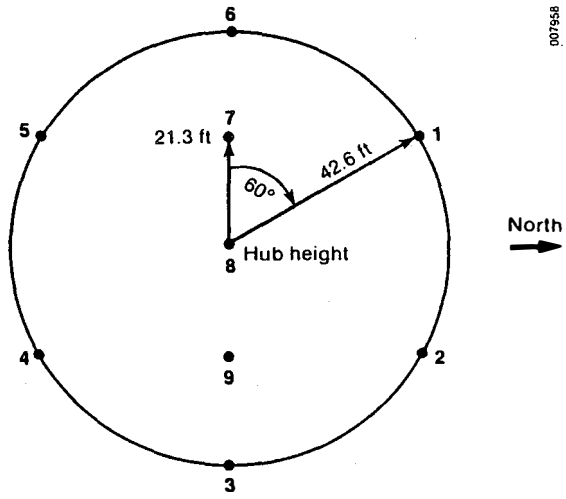

Fig. 3. Placement and numbering of the UVW Gill anemometers on the array (looking upwind to the west)

DATA ANALYSIS

In this study, three different 10-min data segments were prepared for comparison to FLAP code predictions. These cases had different mean wind speeds and turbulence intensities. Table 3 shows the characteristics of the three data sets.

Data case 12-7 had a high turbulence intensity (0.18) compared to the other two cases. In data case 17-1 (the high-wind-speed case), the tip pitch was very active with a mean value of 10.9° and a standard deviation of 4.5°. Data case 17-1 had the same turbulence intensity as case 3-5, with a higher mean wind speed (55.4 ft/s). All cases had small yaw errors, less than 1°.

Table 3. Operating Conditions for the Three Ten-Minute Data Cases

	Data Case (run-segment)		
	3-5	12-7	17-1
Mean wind speed, V_{disk}* (ft/s)	32.3	35.4	55.4
Turbulence intensity ($\sigma/\bar{V}$)**	0.13	0.18	0.13
Tip pitch (deg)			
mean	0.3	0.0	10.9
σ	0.1	0.1	4.5

*$V_{disk} = (V_1 + V_2 + V_4 + V_5)/4$, where V_i = 10-min average

**σ = standard deviation of wind speed or pitch
$\bar{V}$ = mean of hub-height anemometer

TURBULENCE INPUTS TO FLAP

The anemometer data were first prepared for input to the least-squares curve-fitting routine. Only wind-speed components normal to the rotor disk were used in the analysis. The vertical and side-to-side wind components had small mean values and variances compared to the components normal to the rotor disk. For each of the data cases, the residual time-series data for each anemometer of the array were determined. The 10-min average of wind speed $\bar{V}_i$ was determined for each anemometer of the array. The value of $\bar{V}_i$ was then subtracted from the time-series data for the i^{th} anemometer, resulting in the formation of the residual time series for every measurement interval of the recorded data:

$$v_{ni} = V_{ni} - \bar{V}_i$$

where i = 1,2,...,9 and n = each measurement step.

The residual time series at a given time step for each anemometer was then used in the curve-fitting routine. The wind field normal to the rotor disk was assumed to be representable by a series expansion in rotor coordinates r and ψ of the form

$$V_y(r,\psi,t) = V_{y,o}(t) + V_{y,z}(t) r \cos\psi + V_{y,x}(t)\, r \sin\psi + V_{y,rr}(t)(r^2 - 1/2\, R^2) + V_{y,rc}(t)\, r^2 \cos 2\psi + V_{y,rs}(t)$$

where R is the rotor disk radius. The directions x and z are shown in Figure 4. Note that this series included terms up to order 2 P, so that any excitation above two per revolution will not be included in this approximation. For more information on the turbulence model upon which this series expansion is based, see (3).

The above equation depends on the spatial rotor coordinates r and ψ and time t. At each measurement step of the digitized anemometer wind-speed data, a least-squares curve-fitting routine was used to determine the coefficients $V_{y,o}(t)$, $V_{y,z}(t)$,..., $V_{y,rs}(t)$. The original wind-speed data file, of 10-min length, had nine columns of data (for nine anemometers) and 12,500 lines. The data were recorded every 0.048 seconds (corresponding to the 20.84-Hz sampling rate). This file was then converted to one with six columns (corresponding to the six coefficients in the above equation) and 12,500 lines using the least-squares method. This data file containing the curve-fitted coefficients was then input to the FLAP code.

It was assumed that for stationary operating conditions of the turbine, the deterministic and stochastic loads for the turbine test data could be separated by azimuth averaging.

Azimuth-averaged rotor-blade bending moments (test data) were determined by binning the time-series load data with respect to rotor azimuth angle. The stochastic portion of the flapwise-bending-moment test data was determined by subtracting the deterministic azimuth-averaged portion of the load from the bending-moment data. This stochastic portion of load data was then used for comparison to FLAP load predictions. Deterministic load comparisons for this machine were previously shown in (1).

To obtain stochastic FLAP predictions, the FLAP code was then run with zero shear, zero gravity, zero tower shadow, and other deterministic excitations set to zero. Only the mean wind speed and the file containing

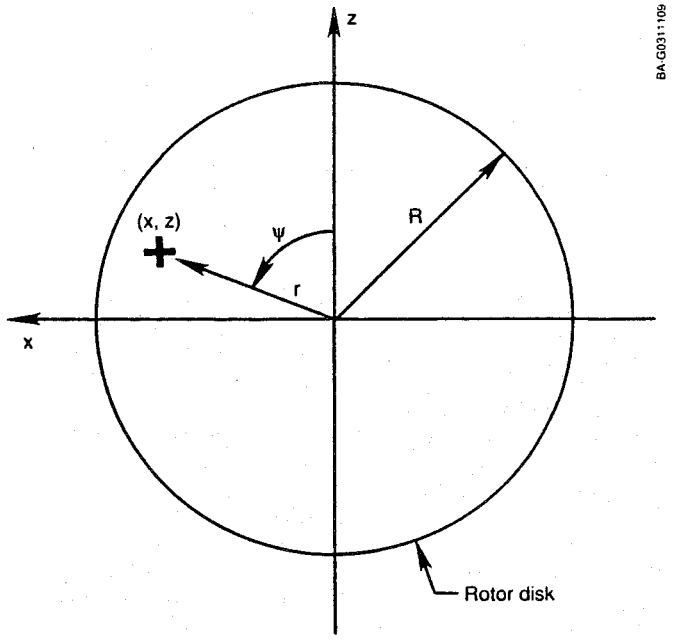

Fig. 4. Rotor disk coordinate system

turbulent wind excitation coefficients were input to the code. The resulting bending-moment predictions contained only the part caused by the response of the blade to the turbulent wind fluctuations. The deterministic response was zero, except for the constant bending load caused by the mean wind, which was simply subtracted from the results. Table 4 compares constant bending loads to measured results for these cases.

Table 4. Comparison of Mean Flapwise Root Bending Moments at Different Mean Wind Speeds: FLAP Prediction Versus Measured Values

Case	Mean Wind Speed (ft/s)	Measured Load (ft-lb)	Predicted Load (ft-lb)
12-7	35.4	45000	37100
17-1	55.4	67500	47500
3-5	32.3	38400	32100

The FLAP code was run in a trim-solution mode first, with the mean wind speed as the principal input to start the solution procedure. After a trim solution was found, the code was run in a transient run condition and coefficients for the wind velocity expansion were read every 0.048 seconds. The FLAP numerical integration procedure uses unequal time steps. For blade positions lying between recorded data measurement intervals, linear interpolation was performed on the estimated coefficients. The equation was then expanded in the aerodynamic subroutines of FLAP to form the correct velocity profile over the rotor disk at any time step.

The induced velocity calculations in the FLAP code were reprogrammed to include the influence of the $V_{y,o}(t)$ term. Thus, the induced velocity calculation was based on the sum of $\bar{V} + V_{y,o}(t)$. The $V_{y,o}(t)$ term was included because the major velocity fluctuation contributions of this term are low-frequency (well below 1 P), and the rotor wake should therefore respond in a quasi-steady manner.

FLAP-predicted flap-bending moments were then output at each interval corresponding to recorded data. Power spectra of predicted flapwise bending moments were then computed and compared to spectra for the measured loads.

DISCUSSION OF RESULTS

To determine the accuracy of the curve-fitting routine, the power spectra of wind speeds generated from the fitted equation were compared to power spectra of actual anemometer time-series data. This comparison assured that the fitted coefficients input to FLAP were accurate.

Figures 5 and 6 show the comparisons between approximation and actual anemometer data for case 12-7 and anemometers #1 and #9. The figures show that the frequency content of the curve-fitted results are underestimated for anemometer #9, for a frequency range of 1-10 rad/s. The fitted results agree well with test data for anemometer #1, which is at the outer edge of the rotor disk. These results are most likely caused by using a greater number of anemometers at the rotor

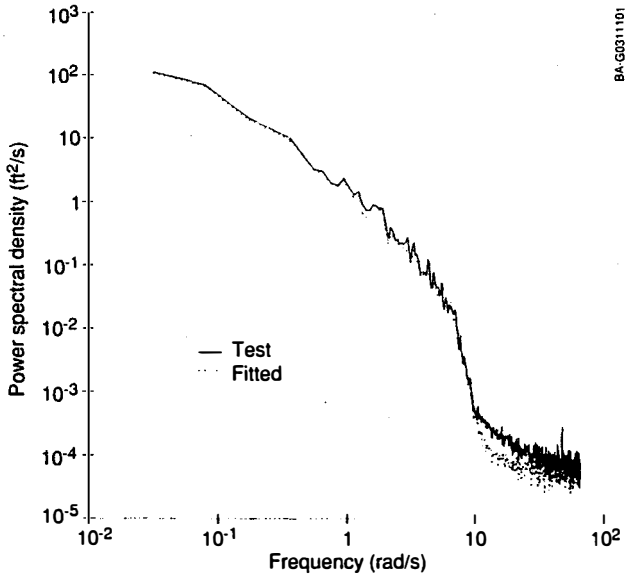

Fig. 5. Comparison of spectra for anemometer #1

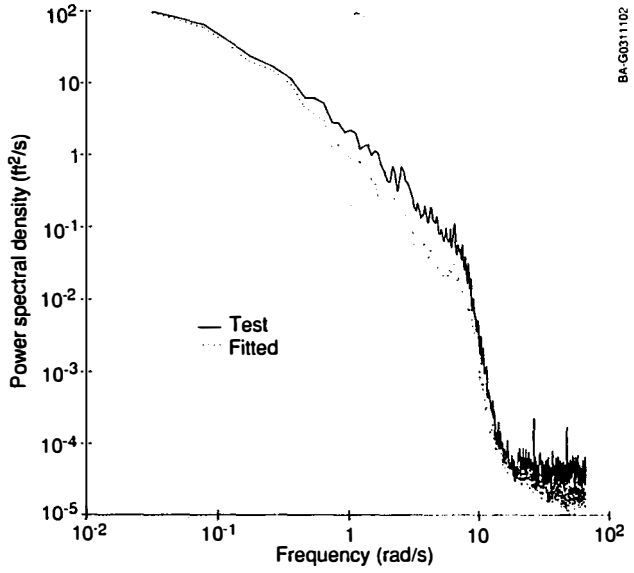

Fig. 6. Comparison of spectra for anemometer #9

disk radius (six) in the curve-fitting routine. Also, the interpolated wind speeds will have the greatest loss of variance at the center of the disk (6). Only three anemometers were used inboard towards the hub. The errors between fitted and measured wind speeds were greater near the hub. As we'll see next, these discrepancies do not seem to cause large discrepancies in the comparisons of flap-bending moments, probably because the inboard airloads on the blade do not contribute a significant amount to the total blade loading.

Figures 7 through 12 present predicted power spectra for flap-bending moments and compare them to test measurements. The three different data cases are shown at two different blade spanwise locations, the 4.9-ft (1.5-m) and 27.1-ft (8.25-m) stations.

Recall that cases 3-5 and 12-7 were for lower wind speeds than was 17-1. Therefore, the tip pitch control was inactive for these cases. Data case 12-7 had the

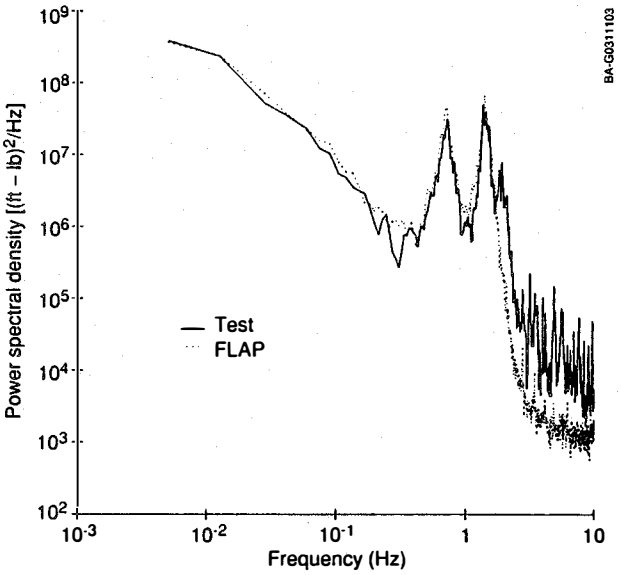

Fig. 7. Spectra of 4.9-ft (1.5-m) flap bending (case 3-5)

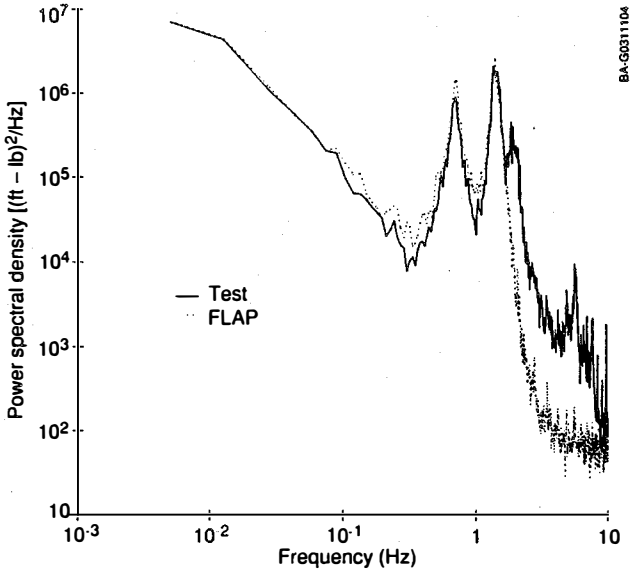

Fig. 8. Spectra of 27.1-ft (8.25-m) flap bending (case 3-5)

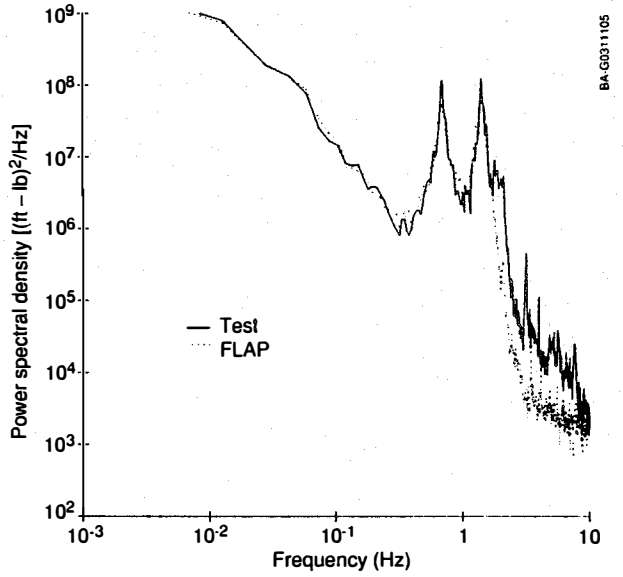

Fig. 9. Spectra of 4.9-ft (1.5-m) flap bending (case 12-7)

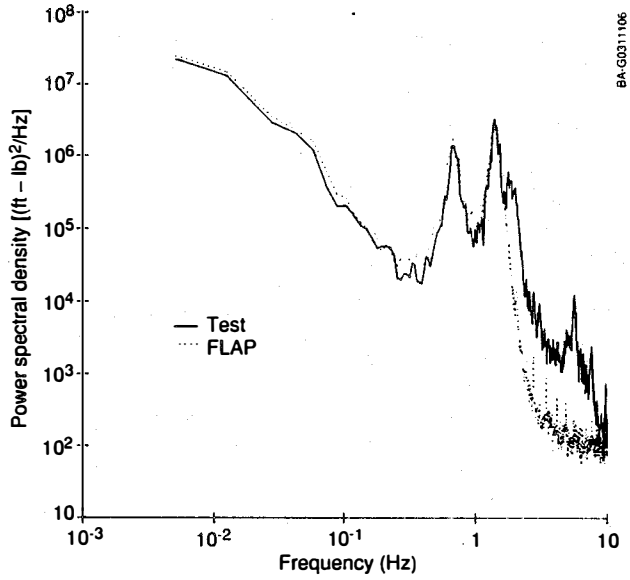

Fig. 10. Spectra of 27.1-ft (8.25-m) flap bending (case 12-7)

highest turbulence intensity (0.18). The FLAP code predictions agree well with test data at both spanwise stations for both cases. The code predicts the two spikes at the 1 P and 2 P (0.7 Hz and 1.40 Hz) frequencies. It also predicts quite well the frequency content below 1 P.

The FLAP code predictions drop off for frequencies immediately above 2 P. This is because the series expansion for the turbulence velocity does not contain any terms for harmonics above 2 P. Thus, the excitation only goes up to 2 P (1.40 Hz). Above the 2 P frequency, the response is caused by tower motion and the second flapwise blade frequency. These responses are also not predicted by FLAP because only one flap-bending mode is used in the code (for this case) and because there is no coupled rotor-tower model. Still, the FLAP code seems to model the most important responses for this rotor for these two data cases (3-5 and 12-7).

For case 17-1, the discrepancy between theory and measurement is most likely from the neglect of blade pitch motion in FLAP. The blade tip pitch was very active for this case. The mean pitch angle was 10.9°, and the standard deviation was 4.5°. Case 17-1 had a low turbulence intensity (0.13). The difference between cases 17-1 and 3-5 was caused by the higher mean wind speed and active pitch for case 17-1. The discrepancies between theory and measurement may be caused by the active blade pitch. Another cause for discrepancy could be that a large portion of the blade is in stall at this wind speed. The mean loads prediction, shown in Table 4, had the largest error for

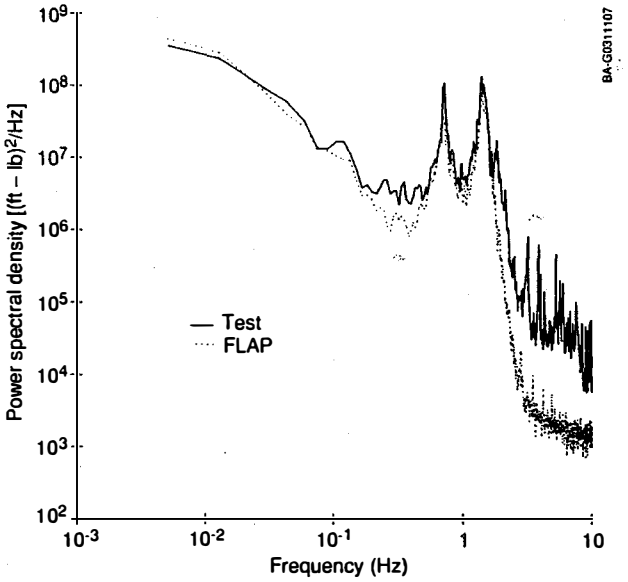

Fig. 11. Spectra of 4.9-ft (1.5-m) flap bending (case 17-1)

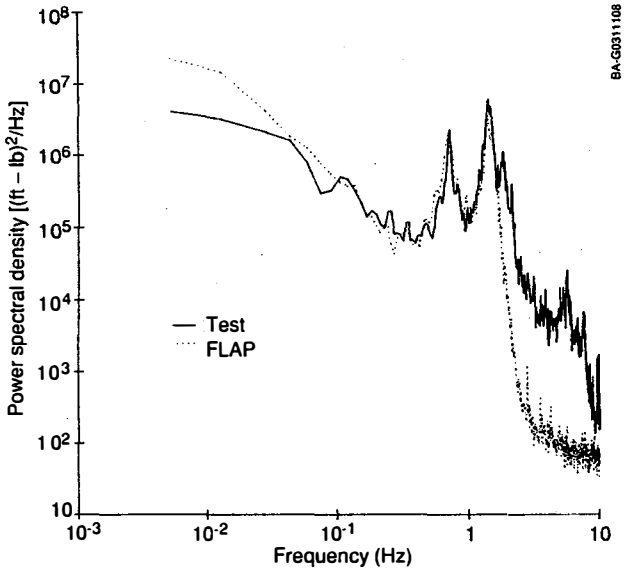

Fig. 12. Spectra of 27.1-ft (8.25-m) flap bending (case 17.1)

case 17-1. The FLAP code does not account for blade stall correctly. It uses simple linear aerodynamics for angles of attack below stall and then sets the lift coefficient equal to the maximum lift coefficient for larger angles of attack (greater than α-stall).

CONCLUSIONS

FLAP code predictions were compared to measured blade flapwise bending moments for three different data cases of the Howden 330-kW turbine. Actual anemometer test data were used as the turbulent wind input to FLAP. An array of nine anemometers was located 0.8 D upwind of the three-bladed, 85.3-ft (26-m)-diameter turbine. Data from each anemometer were used in a least-squares curve-fitting routine to obtain a series expansion of the turbulence field over the rotor disk.

The FLAP code was run with zero shear, zero gravity, and other deterministic excitations set to zero. The only input to FLAP was the mean wind speed and the file containing the turbulent wind expansion coefficients. The resulting FLAP predictions were compared to the stochastic portion of the measured blade bending moments for the three ten-minute data cases and two spanwise locations.

Power spectra of code predictions (using one flap-bending mode) agreed with spectra of measured results for two cases, even at a high turbulence intensity. For the high-wind-speed case, the code predictions deviated from measured results because the actual blade tip pitch was highly active and stall behavior was not modeled correctly. The FLAP code does not now account for time-varying blade pitch.

Other comparison methods should be tried in the future, such as an actual comparison of predicted and measured load time series data rather than just power spectra comparisons. Comparing power spectra between prediction and measurements is only a first step to complete code validation.

Future plans for FLAP code validation and refinement also include comparisons of code turbulent load predictions to measurements for other rotors. Such rotors include the Northern Power Systems teetering rotor, in which extensive data have been collected through cooperative field testing; and machine data collected at SERI during the Combined Experiment. By comparing predictions to test data for other machines, the importance will be ascertained of adding such options as coupled rotor-tower motion and blade chordwise degrees of freedom. Also, the chordwise data from the Howden 330-kW machine will be compared to FLAP predictions.

A general version of the FLAP code (without turbulence) is currently fully documented and in the public domain for use on IBM PC or compatible computers (9). Work is progressing rapidly to make a version available that contains the option of turbulent wind excitation.

The authors would like to suggest that the turbulent wind field for the three data cases used for this comparison could be used by designers for calculating turbulence-induced loads. The wind field expansion equation given earlier could be programmed into virtually any time-domain rotor code. The coefficients $V_{y,o}(t)$, $V_{y,z}(t)$,..., $V_{y,rs}(t)$ for a 10-min data case fit on a single 1.2-Mb floppy disk and can be made available upon request.

ACKNOWLEDGEMENTS

This work could not have been accomplished without the effort of Susan Hock of SERI, who made valuable contributions in analyzing and interpreting the machine test data. Thanks must also be extended to Tom Hausfeld, formerly with SERI, for his many weeks of work at the test site to collect this data set.

REFERENCES

1. Wright, A. D. and Thresher, R. W., "Accurate Rotor Loads Prediction Using the FLAP Dynamics Code," Windpower '87 Proceedings, SERI/CP-217-3315, American Wind Energy Association, Alexandria, Virginia, 1987.

2. Thresher, R. W., Holley, W. E., and Jafarey, N., "Wind Response Characteristics of HAWTS," 1981 Wind Turbine Dynamics Workshop Conference Proceedings, Cleveland, Ohio, February 24-26, 1981.

3. Holley, W. E., Thresher, R. W., and Lin, S. R., "Atmospheric Turbulence Inputs for Horizontal Axis Wind Turbines," Proceedings of the International Wind Energy Conference, 22-26 October 1984, Hamburg, FRG, pp. 443-452.

4. Sharif-Razi, R., Thresher, R. W., and Holley, W. E., Digital Simulation of Turbulence Excitation for Dynamic Analysis of Wind Turbines, March 1985, Oregon State University, Corvallis, Oreg.

5. Madsen, P. H., Hock, S. M., and Hausfeld, T. E., Turbulence Loads on the Howden 26-m-Diameter Wind Turbine, SERI/TP-217-3269, 1987, presented at the 7th ASME Wind Energy Symposium, New Orleans, Louisiana, January 1988, Solar Energy Research Institute, Golden, Colo.

6. Veers, P. S., Three-Dimensional Wind Simulation, SAND88-0152, March 1988, Sandia National Laboratories, Albuquerque, N. Mex.

7. Thresher, R. W., Holley, W. E., and Wright, A. D., "Prediction of Stochastic Blade Responses Using a Filtered Noise Turbulence Model in the FLAP Code," to be presented at the 8th ASME Wind Energy Symposium, Houston, Texas, January 22-26, 1989.

8. Redmond, I., Anderson, C. G., and Jamieson, P., Dynamic Response of a 330-kW Horizontal Axis Wind Turbine Generator, SERI/STR-217-3203, 1988, prepared by James Howden and Company, Ltd., under SERI Cooperative Agreement No. DE-FC02-85CH10249, Solar Energy Research Institute, Golden, Colo.

9. Wright, A. D., Buhl, M. L., and Thresher, R. W., FLAP Code Development and Validation, SERI/TR-217-3125, 1988, Solar Energy Research Institute, Golden, Colo.